Desalination and Water Treatment
www.deswater.com
doi: 10.1080/19443994.2015.1091995

57 (2016) 16096–16103
July

Taylor & Francis
Taylor & Francis Group

Optimization of process variables by dried *Bacillus cereus* for biosorption of nickel(II) using response surface method

Jing Zhang, Tao Yang, Hongyu Wang*, Kai Yang*

School of Civil Engineering, Wuhan University, Wuhan 430072, China, emails: zj220220@126.com (J. Zhang), wuhandaxue220@126.com (T. Yang), hongyuwang220@126.com (H. Wang), Tel. +86 027 61218623; Fax: +86 027 68775328; email: yk220220@126.com (K. Yang)

Received 5 March 2015; Accepted 29 August 2015

ABSTRACT

The biosorption of nickel(II) by dried cells of *Bacillus cereus*, isolated from the sediment from an SBR reactor, was studied by response surface methodology (RSM). In this study, RSM based on central composite rotatable design was used to analyze the combined and individual effects of operating parameters (biomass dose, initial concentration of nickel(II), and pH) on the nickel adsorption capacity by dried *B. cereus* at an ambient temperature. A quadratic polynomial equation was obtained which could predict the amount of adsorbed nickel (II) by dried *B. cereus*. The analysis of variance showed that the effects of pH and biomass dose both had a significant influence on the removal of nickel(II), but the effect of pH was the most significant. The maximum adsorption amount of nickel(II) was found at a pH of 4, biomass concentration of 2.0 g L^{-1}, and initial nickel(II) ion concentration of 150 mg L^{-1}. Under this condition, the maximum adsorption amount of nickel(II) and the maximum adsorption rate were 20.79 mg g^{-1} and 41.44%, respectively. This study indicated that RSM was an effective method for optimizing the biosorption process. Dried *B. cereus* as an eco-friendly biosorbent showed a remarkable performance on the removal of nickel(II).

Keywords: *Bacillus cereus*; Biosorption; Response surface methodology; Central composite rotatable design; Nickel(II)

1. Introduction

The accumulation of toxic heavy metals in surface waters is mainly caused by industrial discharges, domestic sewage, non-point runoff, urban storm runoff, and atmospheric precipitation [1–3]. Due to their difficult biodegradability, toxicity, accumulation in the food chain, and persistence in nature, heavy metals have been a serious threat to the environment, and the health of animals and mankind [3–5]. According to the World Health Organization (WHO), nickel is one of the most common toxic metals which may benefit organisms at trace amounts as a trace element, but excessive intake of nickel can result in different types of diseases such as pulmonary fibrosis, lung cancer, renal edema, skin dermatitis, and gastrointestinal disorder [2,6]. The US Environmental Protection Agency (EPA) has established 0.5 mg L^{-1} as the permissible concentration for nickel in drinking water [2,7]. Methods commonly used to remove nickel include precipitation, ion exchange, electrochemical processes, and membrane processes [7–9]. However,

*Corresponding authors.

many of these methods are neither effective nor economical, especially when they are used for the removal of heavy metal ions to a low concentration. Therefore, the need for an effective method for the removal of heavy metals from wastewater to attain today's toxicity-driven limits is very crucial.

In recent years, many researches have indicated that biosorption is a cheap, effective, and eco-friendly technique for the removal of heavy metals. In fact, biosorption is a method which uses certain types of inactive, dead microbial biomass (algae, yeast, fungi, and bacteria) to bind and concentrate the heavy metals from wastewater [6,10]. The function of adsorption for those biosorbents is mainly attributed to the presence of a series of surface functional groups on their cell wall, such as carboxylic acid (–COOH), aldehyde (–COH), hydroxyl (–CHOH), sulfhydryl (–SH), phosphoryl (PO_4H_3), and amine ($–NH_2$) organic compounds, which enable those biosorbents to bind metal ions from the liquid phase [11]. Due to easy handling, no nutrient requirements, low costs, and no effect by the toxicity of the metal ions, nonliving biomass is usually used as a cheap, effective, and eco-friendly biosorbent to remove heavy metals from wastewater in practical applications.

Many studies have shown that the biosorption of heavy metal ions by biosorbents is strongly dependent upon the initial concentration of nickel and adsorption conditions [12,13]. And in assessing the effect (single effect and interactive effects) of variables on quality attributes, an adequate experimental design is required. As we all know, response surface methodology (RSM) has an important application for analyzing the effects of several independent variables and interactive effects among the variables on the response [14–16]. Nevertheless, to the best of our knowledge, few of the studies investigated the optimization of adsorption of nickel ions using nonliving *Bacillus cereus* cells by RSM [17]. The aim of the present work is to study the performance of nonliving *B. cereus* cells in removing nickel ions from aqueous solution. The effect of biomass dose , initial concentration of nickel ions, and initial pH was investigated to optimize the removal of nickel ions. This process was analyzed using MATLAB for RSM. Empirical model-correlating response to the three variables was then developed. At last, the biosorbent was characterized through FTIR to know the physicochemical properties of the biosorbent.

2. Materials and methods

2.1. Preparation of adsorbent

B. cereus was isolated from the sediment from an SBR reactor. The isolated bacteria were cryopreserved in a solid medium at 4°C. At the beginning of the experiment, the bacteria were transferred to a 500-mL conical flask containing 300 mL of culture medium (1.2 g of beef extract, 4.0 g of peptone, and 2.0 g of NaCl), and shaken at 150 rpm and 30°C for 48 h, and then harvested by centrifugation at 9,000 rpm and 4°C for 5 min. It was washed with distilled water, dried at 60°C for 12 h, then ground, and sieved into different fractions. The 0.56–0.85 mm particle size fraction was used in the experiments.

2.2. Nickel ion solution standards

The nickel ion solution was prepared from its chloride salt ($NiCl_2{\cdot}6H_2O$). Standard stock solution was prepared in distilled water, slightly acidified with 1 N HCl and 1 N NaOH, and sterilized at 121°C for 15 min, then kept at 25°C. The glassware was leached in 3 N HCl and rinsed several times with distilled water before using, to avoid metal contamination.

2.3. Analysis and measurements

The concentrations of residual nickel ions in the supernatant solutions were determined by dimethylglyoxime spectrophotometric method using UV–vis spectrophotometry (SP-1920, China). The adsorption amount of nickel from the liquid phase was determined at the beginning c_i (mg L^{-1}) and at the end c_f (mg L^{-1}). The following equation was used to compute the biosorbent uptake capacity q (mg g^{-1}), where v (mL) is the volume of the solution and w (g) is the mass of the biosorbent [18]:

$$q = (c_i - c_f) \times \frac{v}{1000\,w} \tag{1}$$

2.4. Experimental design

RSM is a statistical technique used for multiple regression analysis of quantitative data obtained from statistically designed experiments by solving the multivariable equations simultaneously [19]. The central composite design (CCD) is frequently used under RSM design [20]. The adsorbed nickel(II) amount was statistically modeled and designed by RSM. And due to its suitability to fit the quadratic surface which usually works well for process optimization, the CCD was used to optimize the biosorption process.

This design consists of full factorial or fractional factorial design to determine the effects of variables and interactions and an additional design, often a star design, in which the experimental points are at α

distance from its center which can be used to determine the quadratic terms and central point to determine the curvature of response. A central composite rotatable design (CCRD) for three factors was employed for this experimental design to provide data to model the effects of the independent variables such as pH, biomass concentration (g L^{-1}), and initial lead concentration (ppm). The four-factor three-level design, as shown in Table 1, was used for the optimization procedure. The second-order quadratic equation to predict the maximum adsorbed nickel(II) amount is given below:

$$Y = \beta_0 + \sum_{i=1}^{k} \beta_i X_i + \sum_{i=1}^{k} \beta_{ii} X_i^2 + \sum \sum_{i<j=1}^{k} \beta_{ij} X_i X_j + \varepsilon \quad (2)$$

where Y is the predicted response, X_i, X_j, …, X_k are the input variables which affect the response Y, X_i^2 X_j^2, …, X_k^2 are the square effects, X_iX_j and X_jX_k are the interaction effects, β_0 is the intercept term, β_i (i = 1, 2, …, k) is the linear effect, β_{ii} (i = 1, 2, …, k) is the squared effect, β_{ij} (i = 1, 2, …, k; j = 1, 2, …, k) is the interaction effect, and ε is a random error [18,20].

The analysis of variance (ANOVA) data were computed by MATLAB in order to obtain the interaction between the processed variables and the response. The quality of the fit of the polynomial model was expressed by the coefficient of determination (R^2) and the statistical significance was checked by the F test using the same program.

2.5. Characterization of the biosorbent

Characterization of biosorbent surface holds a key to understanding the metal binding mechanism onto biomass. FTIR spectrum of the adsorbent could show the functional groups on the surface of dried cells of *B. cereus* which are responsible to sequester the metal ions from aqueous solution. In this study, the infrared spectrum of nature and metal-laden adsorbents was obtained by the use of a Fourier transform infrared (FTIR) spectrometer (Perkin–Elmer Spectrum 100 FTIR Spectrometer) equipped with an attenuated total reflection (ATR) accessory (Perkin Elmer) to identify the functional groups responsible for the sorption.

3. Result and discussion

3.1. Experimental design

Experimental designs of CCRD with their corresponding results and the percentage removal (experimental and predicated) for the process response are presented in Table 2. The second-order equation for the estimation of the adsorbed nickel(II) amount in terms of pH (X_1), biosorbent dosage (X_2), and initial concentration of nickel(II) (X_3) is represented in terms of coded factors ($-\alpha$, −1, 0, and +1, $+\alpha$) as follows:

$$\begin{aligned}\text{Adsorbed nickel(II) amount (mg g}^{-1}) &= -84.4147 + 13.2048\,X_1 + 15.5378\,X_2 + 0.8475\,X_3 \\ &\quad + 0.4477\,X_1X_2 + 0.0222\,X_2X_3 + 0.0235\,X_2X_3 \\ &\quad - 2.2065\,X_1^2 - 5.2085\,X_2^2 - 0.0033\,X_3^2\end{aligned} \quad (3)$$

Eq. (3) represents the quantitative effect of the process variables (X_1, X_2, and X_3) and their interactive effects on the response (Y). A positive sign in the equation represents a synergistic effect of the variables, while a negative sign indicates an antagonistic effect of the variables. The results of the ANOVA for the proposed statistical model and their model coefficients are given in Tables 3 and 4, respectively.

The F-value, which is a ratio of the mean square due to regression to the mean square due to error, is converted into its corresponding p-value. From the statistical point of view, if p-value < 0.05, then the model is statistically significant. As the p-value decreases, it becomes less likely that the effect is due to a chance and more likely that there was a real cause. In this case, the p-value of model is 0.0001 and it is significant. Besides, R^2 = 0.886 for Eq. (2) indicates a good fitting for the experimental data and predicted values.

Table 1
Independent variable and levels used for CCRD in Ni(II) biosorption process

		Levels				
Variables	Symbols	−1.682 (−α)	−1	0	1	1.682 (α)
pH	X_1	2.00	2.81	4.00	5.19	6.00
Biomass concentration (g L^{-1})	X_2	0.40	1.05	2.00	2.95	3.60
Initial Ni^{2+} concentration (mg L^{-1})	X_3	100.00	120.27	150.00	179.73	200.00

Table 2
CCRD arrangement and responses for the biosorption process

Run	Point type	Factors			Adsorbed amount of Ni ion (ppm)	Nickel ion removal (mg g^{-1})	
		X_1	X_2	X_3		Experimental	Predicted
1	Fact	2.81	1.05	120.27	15.32	12.131	12.226
2	Fact	2.81	2.95	179.73	42.12	7.944	9.763
3	Fact	5.19	2.95	179.73	48.42	9.132	11.834
4	Fact	5.19	2.95	120.27	26.27	7.404	8.844
5	Fact	2.81	2.95	120.27	27.62	7.785	9.920
6	Fact	5.19	1.05	120.27	10.29	8.148	9.126
7	Fact	2.81	1.05	179.73	15.21	8.060	9.416
8	Fact	5.19	1.05	179.73	16.61	8.802	9.463
9	Axial	4	2	200	60.90	15.225	12.685
10	Axial	4	0.4	150	4.75	7.917	7.431
11	Axial	4	2	100	27.9	13.950	12.534
12	Axial	2	2	150	42.80	14.167	12.394
13	Axial	4	3.6	150	59.10	10.944	7.486
14	Axial	6	2	150	40.88	13.627	11.534
15	Center	4	2	150	62.98	20.993	20.792
16	Center	4	2	150	62.10	20.700	20.792
17	Center	4	2	150	60.85	20.283	20.792
18	Center	4	2	150	61.56	20.520	20.792

3.2. Effect of parameter

Each contour in the response surface plot represents one variable maintained at zero levels and a number of combinations of the other two variables, and these studies reveal the best optimal values for the biosorption process.

As shown in Fig. 1(a) and (b), the pH has a significant effect on the adsorption of nickel(II). The adsorbed amount of nickel(II) increased with an increase in the pH from 2 to 4 and approximately reached the maximum around 4, but beyond this pH, the adsorption capacity decreased with an increase in the pH. This phenomenon could be explained using the fact that as the pH increases, the proton concentration decreased and the electrostatic repulsion between the metal cations and the surface also decreased [21,22]. When the pH was beyond 4, as the pH is increasing, the formation of anionic hydroxide complexes decreased the dissolved metal concentration in solution.

Initial nickel(II) concentration is also an important influencing factor. As shown in Fig. 1(b) and (c), the adsorbed amount of nickel(II) rapidly increased with an increase in the initial nickel(II) concentration from 100 to 150 mg L^{-1} and roughly reached the maximum at 150 mg L^{-1}. At low ion concentrations, due to the high ratio of surface active sites to the total metal ions in the solution, the metal ions could interact with the adsorbent and could be removed. To some extent, an increase in the initial ion concentration increases the collision probability between ions and biosorbent, and the metal ions have more chance to interact with the adsorbent which results in the high adsorbed nickel(II) amount . Besides, an increase in the initial ion concentration could provide a larger driving force to overcome the mass transfer resistance between the biosorbent and biosorption medium [22]. However, when the initial ion concentration continued to

Table 3
Regression coefficients of predicted quadratic polynomial

Terms	Regression coefficients
Intercepts	
β_0	−84.4147
Linear term	
β_1	13.2048
β_2	15.5378
β_3	0.8475
Quadratic	
β_{11}	−0.4477
β_{22}	−0.0222
β_{33}	−0.0235
Interaction	
β_{12}	−2.2065
β_{13}	−5.2085
β_{23}	−0.0033

Table 4
ANOVA for the adsorbed nickel(II) amount model

	Sum of squares	df	Mean square	*F*-value	*p*-value	R^2	
Model	384.537	1	384.537	124.535	0.000	0.886	Significant
Residual	49.405	16	3.088				
Total	433.942	17					

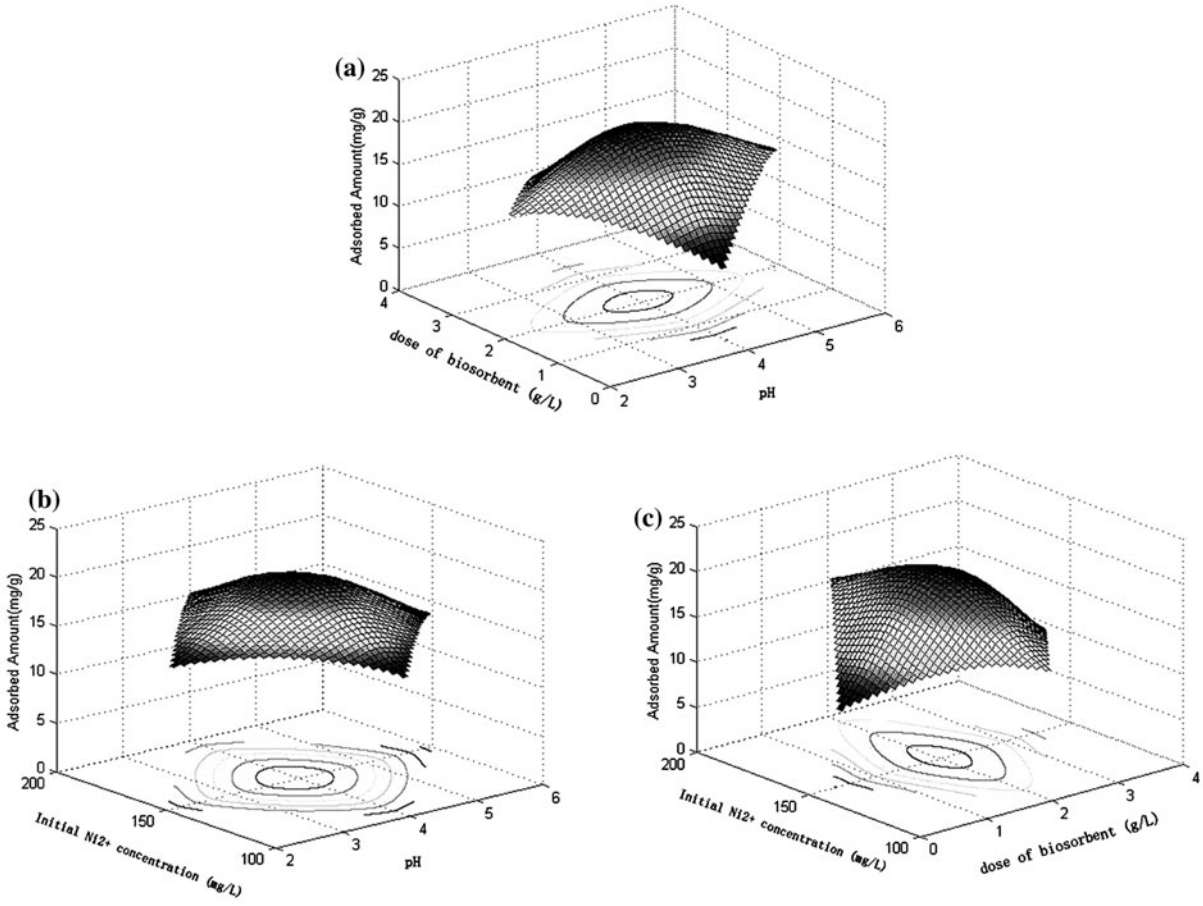

Fig. 1. Response surface plot showing the simultaneous effects of (a) pH and biosorbent dosage, (b) pH and initial nickel(II) concentration, and (c) biosorbent dosage and initial nickel(II) concentration on the adsorbed nickel(II) amount.

increase, the metal uptake reached equilibrium and all sites were almost saturated with metals, so the rate of increment of adsorption capacity became gradually slower [2,16].

Fig. 1(a) and (c) shows the effect of biosorbent concentration on the adsorbed amount of nickel(II). It was observed from Fig. 1(a) and (c) that the adsorbed amount of nickel(II) highly depended on the increase in the biosorbent concentration, and when the biosorbent concentration reached around 2.0 g L^{-1}, the maximum biosorption (20.79 mg g^{-1}) of the metal ions was attained. The biosorption of nickel(II) is proportional to the binding sites. The higher dose of biosorbent in the solution leads to the greater availability of exchangeable sites for the ions. However, the adsorbed nickel(II) amount decreased when the biomass dosages were beyond 2.0 g L^{-1}. This behavior was attributed to a partial aggregation of biomass which reduces the availability of exchangeable sites for the biosorption [11].

3.3. The simultaneous effects of parameter

Fig. 1(a–c) was drawn at a constant value of 150 mg L^{-1} initial nickel concentration (X_3), 2.0 g L^{-1} biomass concentration (X_2), and pH (X_1) = 4, respectively. Fig. 1(a–c) shows the simultaneous effects of pH and biosorbent dosage, the simultaneous effects of pH and initial nickel(II) concentration, and the simultaneous effects of biosorbent dosage and initial nickel(II) concentration on the adsorbed nickel(II) amount, respectively.

By comparing Fig. 1(b) and (c) at the same initial nickel(II) concentration, the pH varied from 2 to 4 with 150 rpm for 4 h at 30°C and the adsorbed nickel(II) amount increased from 14.54 to 20.79 mg g^{-1}. Similarly, under the same conditions, Fig. 1(b) shows that when the biosorbent dosage varied from 2 to 2.25 g L^{-1}, the adsorbed nickel(II) amount increased from 8.46 to 20.79 mg g^{-1}. When the pH varied from 4 to 6, the adsorbed nickel(II) amount decreased from 20.79 to 14.22 mg g^{-1}. While the biosorbent dosage increased from 2 to 2.25 g L^{-1}, the adsorbed nickel(II) amount decreased from 20.79 to 11.85 mg g^{-1}. It is very clearly indicated that the effect of the biosorbent dosage is greater than that of pH.

In the same way, as shown in Fig. 1(a) and (c), the volatility of the adsorbed nickel(II) amount by the variation of initial nickel(II) concentration was lower than that by the variation of the pH, so the effect of the former was lower than that of the latter. And Fig. 1(b) and (c) clearly shows the effect on the adsorbed nickel(II) amount by the variation of initial nickel(II) concentration which was lower than that by the variation of biosorbent dosage. However, from Fig. 1, the interaction of X_1X_2 was the most significant and the interaction of X_2X_3 was the most insignificant. From Eq. (3), the coefficient of X_1X_2, X_1X_3, and X_2X_3 was 0.8475, 0.4433, and 0.0222, respectively. This also illustrated that the term of X_1X_2 has more effect than other terms.

3.4. Evaluation of the optimum adsorption conditions

The objective of the experimental design was to optimize the process conditions for maximizing the adsorbed nickel(II) amount. The optimum points of the parameters to maximize the adsorption of nickel(II) were evaluated by the application of Eq. (3). From Eq. (3), the optimum values for adsorbed nickel(II) amount were 150 mg L^{-1}, 4, and 2.0 g L^{-1} for initial nickel(II) concentration, pH, and biosorbent dosage, respectively. Under optimum conditions, the adsorbed amount was 20.79 mg g^{-1} and the corresponding removal efficiency of nickel(II) was 41.44%. These results were confirmed with experiments (20.52 mg g^{-1}).

3.5. Infrared spectroscopy

FTIR spectrum of unloaded and Ni^{2+}-loaded by nonliving *B. cereus* is shown in Fig. 2. These results represented the information about the functional groups on the surface of the cell wall of the biomass and the possible interaction between metals and the functional groups. The spectra of unloaded biomass indicated several major bands around 1,059, 1,232, 1,345, 1,453, 1,529, 1,656, 2,925, and 3,288 cm^{-1}. The peaks in the region of wave numbers 3,288.31–3,427.83 cm^{-1} reflected the overlapping between N–H and O–H stretching vibrations. The peak observed at about 2,922 cm^{-1} was assigned to the stretching vibrations of the C–H bond of methylene groups. The peak at about 1,653 cm^{-1} was due to the stretching band of carboxyl groups. The band at 1,549.28 cm^{-1} could be assigned to a combination of the stretching vibration of C–N and deformation vibration of N–H peptidic bond of protein (Amide II). The peaks in the range 1,470–1,330 cm^{-1} were representatives of amino-substituted alkyl group. The band at 1,231.05 cm^{-1} could be attributed to the C–N stretching of Amide III, while the band at 1,059.79 cm^{-1} could be attributed to the stretching vibration of O–H of polysaccharides [23–25]. Meanwhile, some bands in the fingerprint region could be related to the phosphate groups.

After nickel(II) binding, a change of peak positions was observed at 1,529, 1,656, 2,925, and 3,288 cm^{-1}. As shown in the Fig. 2, at 1,529, 1,656, 2,925, and 3,288 cm^{-1}, T% shifted from 53.5, 43.3, 66.4, and 56.8% to 65.7, 58.9, 73.1, and 66.5%, respectively. The significant changes in the wave number of these peaks after loading of nickel(II) indicated that the functional groups (C–N, N–H, carboxyl groups, C–H, hydroxyl, and O–H) were involved in the biosorption of nickel(II) on the surface of *B. cereus*.

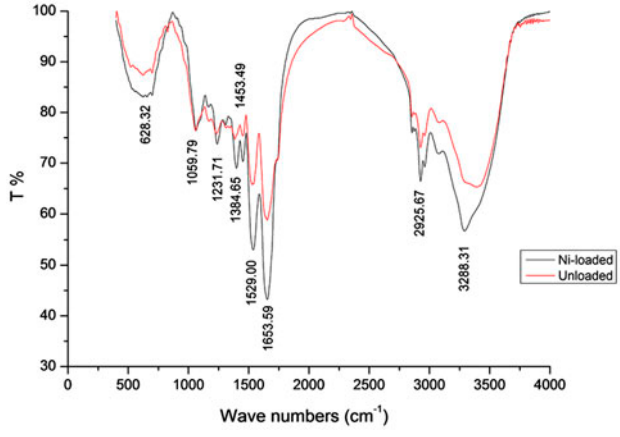

Fig. 2. FT-IR spectra of unloaded and Ni-loaded.

4. Conclusions

In this study, the biosorption of nickel(II) by dried *B. cereus* had been investigated. The RSM combined with CCD and MATLAB 7.11 was used to study the effects of the operating variables (pH, biomass dosage, and initial nickel concentration) on the adsorbed nickel(II) amount. And the obtained second-order polynomial equation model, whose validity was agreed upon, was estimated using the ANOVA statistical testing. The optimum biosorption condition obtained by CCD design was a pH of 4, biomass concentration of 2.0 g L^{-1}, and initial nickel(II) concentration of 150 mg L^{-1}. The optimum-adsorbed nickel(II) amount and the optimum adsorption efficiency were 20.79 mg g^{-1} and 41.44%, respectively. The experimental results showed pH and biomass dosage both played a significant effect on the adsorption of nickel(II) by dried cells *B. cereus*, but the effect of pH was the most significant. Based on these results, it could be concluded that dried *B. cereus* could be used as a potential biosorbent for the removal of nickel(II) from aqueous solution.

Acknowledgments

This research was financially supported by the National Natural Science Foundation of China (NSFC) (No. 51378400), the National Science and Technology Pillar Program (2014BAL04B04), and the Natural Science Foundation of Hubei Province, China (numbers 2013CFB289; 2013CFB308).

References

[1] M. Riaz, R. Nadeem, M.A. Hanif, T.M. Ansari, K. Rehman, Pb(II) biosorption from hazardous aqueous streams using *Gossypium hirsutum* (Cotton) waste biomass, J. Hazard. Mater. 161(1) (2009) 88–94.

[2] V.K. Gupta, A. Rastogi, A. Nayak, Biosorption of nickel onto treated alga (*Oedogonium hatei*): Application of isotherm and kinetic models, J. Colloid Interface Sci. 342(2) (2010) 533–539.

[3] D.H.K. Reddy, D.K.V. Ramana, K. Seshaiah, A.V.R. Reddy, Biosorption of Ni(II) from aqueous phase by *Moringa oleifera* bark, a low cost biosorbent, Desalination 268(1–3) (2011) 150–157.

[4] A. Çelekli, M. Yavuzatmaca, H. Bozkurt, An eco-friendly process: Predictive modelling of copper adsorption from aqueous solution on *Spirulina platensis*, J. Hazard. Mater. 173(1–3) (2010) 123–129.

[5] R. Flouty, G. Estephane, Bioaccumulation and biosorption of copper and lead by a unicellular algae *Chlamydomonas reinhardtii* in single and binary metal systems: A comparative study, J. Environ. Manage. 111 (2012) 106–114.

[6] A. Çelekli, H. Bozkurt, Bio-sorption of cadmium and nickel ions using *Spirulina platensis*: Kinetic and equilibrium studies, Desalination 275(1–3) (2011) 141–147.

[7] H. Pahlavanzadeh, A.R. Keshtkar, J. Safdari, Z. Abadi, Biosorption of nickel(II) from aqueous solution by brown algae: Equilibrium, dynamic and thermodynamic studies, J. Hazard. Mater. 175(1–3) (2010) 304–310.

[8] A. Demirbas, Heavy metal adsorption onto agro-based waste materials: A review, J. Hazard. Mater. 157(2–3) (2008) 220–229.

[9] M.V. Subbaiah, Y.S. Yun, Biosorption of Nickel(II) from aqueous solution by the fungal mat of *Trametes versicolor* (rainbow) biomass: Equilibrium, kinetics, and thermodynamic studies, Biotechnol. Bioprocess Eng. 18(2) (2013) 280–288.

[10] R.A. Anayurt, A. Sari, M. Tuzen, Equilibrium, thermodynamic and kinetic studies on biosorption of Pb(II) and Cd(II) from aqueous solution by macrofungus (*Lactarius scrobiculatus*) biomass, Chem. Eng. J. 151 (1–3) (2009) 255–261.

[11] Y. Zhang, C. Banks, A comparison of the properties of polyurethane immobilised *Sphagnum* moss, seaweed, sunflower waste and maize for the biosorption of Cu, Pb, Zn and Ni in continuous flow packed columns, Water Res. 40(4) (2006) 788–798.

[12] S.E. Oh, S.H.A. Hassan, J.H. Joo, Biosorption of heavy metals by lyophilized cells of *Pseudomonas stutzeri*, World J. Microbiol. Biotechnol. 25(10) (2009) 1771–1778.

[13] R.M. Gabr, S.M.F. Gad-Elrab, R.N.N. Abskharon, S.H.A. Hassan, A.A.M. Shoreit, Biosorption of hexavalent chromium using biofilm of *E. coli* supported on granulated activated carbon, World J. Microbiol. Biotechnol. 25(10) (2009) 1695–1703.

[14] M. Amini, H. Younesi, N. Bahramifar, A.A.Z. Lorestani, F. Ghorbani, A. Daneshi, M. Sharifzadeh, Application of response surface methodology for optimization of lead biosorption in an aqueous solution by *Aspergillus niger*, J. Hazard. Mater. 154(1–3) (2008) 694–702.

[15] J. Aravind, C. Lenin, C. Nancyflavia, P. Rashika, S. Saravanan, Response surface methodology optimization of nickel(II) removal using pigeon pea pod biosorbent, Int. J. Environ. Sci. Technol. 12(1) (2015) 105–114.

[16] S. Murugesan, S. Rajiv, M. Thanapalan, Optimization of process variables for a biosorption of nickel(II) using response surface method, Korean J. Chem. Eng. 26(2) (2009) 364–370.

[17] Z.M. Bahari, W.A.H. Altowayti, Z. Ibrahim, J. Jaafar, S. Shahir, Biosorption of As(III) by non-living biomass of an arsenic-hypertolerant *Bacillus cereus* strain SZ2 isolated from a gold mining environment: Equilibrium and kinetic study, Appl. Biochem. Biotechnol. 171(8) (2013) 2247–2261.

[18] T. Şahan, D. Öztürk, Investigation of Pb(II) adsorption onto pumice samples: Application of optimization method based on fractional factorial design and response surface methodology, Clean Technol. Environ. Policy 16(5) (2014) 819–831.

[19] S.K. Ponnusamy, R. Subramaniam, Process optimization studies of Congo red dye adsorption onto cashew nut shell using response surface methodology, Int. J. Ind. Chem. 4(1) (2013) 1–10.

[20] H. Turkyilmaz, T. Kartal, S.Y. Yildiz, Optimization of lead adsorption of mordenite by response surface methodology: Characterization and modification, J. Environ. Health Sci. Eng. 12(1) (2014) 5, doi:10.1186/2052-336X-12-5.
[21] A. Suazo-Madrid, L. Morales-Barrera, E. Aranda-García, E. Cristiani-Urbina, Nickel(II) biosorption by *Rhodotorula glutinis*, J. Ind. Microbiol. Biotechnol. 38(1) (2011) 51–64.
[22] G. Edris, Y. Alhamed, A. Alzahrani, Biosorption of cadmium and lead from aqueous solutions by *Chlorella vulgaris* biomass: Equilibrium and kinetic study, Arabian J. Sci. Eng. 39(1) (2014) 87–93.
[23] Y. Tang, L. Chen, X. Wei, Q. Yao, T. Li, Removal of lead ions from aqueous solution by the dried aquatic plant, *Lemna perpusilla* Torr, J. Hazard. Mater. 244 (2013) 603–612.
[24] A.M.A. Aty, N.S. Ammar, H.H.A. Ghafar, R.K. Ali, Biosorption of cadmium and lead from aqueous solution by fresh water alga *Anabaena sphaerica* biomass, J. Adv. Res. 4(4) (2013) 367–374.
[25] J. Gao, Q. Zhang, J. Wang, X. Wu, S. Wang, Y. Peng, Contributions of functional groups and extracellular polymeric substances on the biosorption of dyes by aerobic granules, Bioresour. Technol. 102(2) (2011) 805–813.